

# Relations between Static and Dynamic Moduli of Sedimentary Rocks

Erling Fjær

SINTEF Petroleum Research

and Norwegian University of Science and Technology

Trondheim, Norway

[erling.fjaer@sintef.no](mailto:erling.fjaer@sintef.no)

Keywords:

- Dispersion
- Static and dynamic moduli

## ABSTRACT

Static moduli of rocks are usually different from the corresponding dynamic moduli. The ratio between them is generally complex and depends on several conditions, including stress state and stress history. Different drainage conditions, dispersion - often associated with pore fluid effects – heterogeneities and strain amplitude are all potential reasons for this discrepancy. Moreover, comparison of static and dynamic moduli is often hampered and maybe mistaken due to insufficient characterization of anisotropy.

This paper gives a review of the various mechanisms causing differences between static and dynamic moduli. By careful arrangements of test conditions, it is possible to isolate the mechanisms so that they can be studied separately. Non-elastic deformation induced by the large static strain amplitudes is particularly challenging, however a linear relationship between non-elastic compliance and stress makes it possible to eliminate also this effect by extrapolation to zero strain amplitude.

To a large extent, each mechanism can be expressed mathematically with reasonable precision, thus quantitative relations between the moduli can be established. This provides useful tools for analyses and prediction of rock behavior. For instance, such relations may be used to predict static stiffness and even strength based on dynamic measurement. This is particularly useful in field situations where only dynamic data are available. Further, by utilizing the possibility for extrapolation of static measurements to zero strain amplitude, dispersion in the range from seismic to ultrasonic frequencies may be studied by a combination of static and dynamic measurements.

## 1 INTRODUCTION

Within geo-science and -engineering it is customary to differentiate between static and dynamic elastic moduli. The term "dynamic moduli" usually refers to the elastic stiffness that can be derived from elastic wave velocities in combination with density. "Static moduli" on the other hand refers to the elastic stiffness that relates deformation to applied stress in a quasi-static loading situation, i.e. the slope of the stress-strain curve.

For an isotropic material, the dynamic bulk modulus ( $K_{dyn}$ ) and Young's modulus ( $E_{dyn}$ ) can be expressed as functions of the P- and S-wave velocities ( $V_P$  and  $V_S$ , respectively) and the density  $\rho$ :

$$K_{dyn} = \rho \left( V_P^2 - \frac{4}{3} V_S^2 \right) \quad (1)$$

$$E_{dyn} = \rho V_S^2 \frac{3V_P^2 - 4V_S^2}{V_P^2 - V_S^2} \quad (2)$$

The static bulk modulus ( $K_{stat}$ ) and Young's modulus ( $E_{stat}$ ) can be found as the ratio between hydrostatic stress ( $\sigma$ ) and volumetric strain ( $\varepsilon_{vol}$ ) increments in a hydrostatic test, or the ratio between axial stress ( $\sigma_z$ ) and axial strain ( $\varepsilon_z$ ) increments in a uniaxial test, respectively:

$$K_{stat} = \frac{\Delta \sigma}{\Delta \varepsilon_{vol}} \quad (3)$$

$$E_{stat} = \frac{\Delta \sigma_z}{\Delta \varepsilon_z} \quad (4)$$

Within the frame of linear elasticity, isotropy and homogeneity, corresponding components of static and dynamic moduli are equal, i.e.  $K_{stat} = K_{dyn}$  and  $E_{stat} = E_{dyn}$ . This may be valid for a homogeneous material like steel (Ledbetter 1993). However, for rocks there can be large differences between static and dynamic moduli, and the dynamic stiffness is almost always larger than the static one (Simmons and Brace 1965; Walsh 1965; King 1970; Cheng and Johnston 1981; Jizba and Nur

1990; Martin and Haupt 1994; Yale and Jamieson 1994; Tutuncu et al. 1998; Fjær 1999, 2009, Olsen, Christensen and Fabricius 2008). There are several potential reasons for these differences, as listed below. Strain rate is one of them, however it is not necessarily the most important one although the labels "static" and "dynamic" may indicate otherwise.

The most relevant causes for differences between static and dynamic moduli of rocks are:

1. **Strain rate.** Given the labels "static" and "dynamic" moduli, it is natural to assume that the major explanation for the discrepancy between the two is given by the difference in deformation rate induced by elastic waves versus that of "static" loading. However, the strain rate induced during a typical rock mechanical laboratory test corresponds to the strain rate of an elastic wave in the lower end of the seismic frequency band (Fjær, Stroisz and Holt 2013). Thus, with respect to strain rate, dynamic moduli derived from seismic waves may be closer to static moduli from a laboratory test than to dynamic moduli derived from ultrasonic waves.
2. **Drainage conditions.** It is well known from poroelastic theory (Gassmann 1951; Biot 1955, 1956a) that there may be large differences in stiffness whether the rock is drained or undrained. The deformations induced by elastic waves in a fully saturated rock are always undrained, while "static" deformations are often drained. Thus, a difference in drainage conditions is also a possible cause for differences between static and dynamic moduli.
3. **Heterogeneities.** Heterogeneities of different scales are a natural property of rocks. While comparing static and dynamic moduli, it is therefore essential to keep in mind that the elastic waves may not probe exactly the same rock volume as the static load. For largely heterogeneous rocks, this is clearly a potential cause for a difference between static and dynamic moduli.
4. **Anisotropy.** Rock stiffness is in general, for orthorhombic symmetry, a tensor with 9 independent components. Thus, while comparing static and dynamic moduli, it is essential that we compare the same components, and that anisotropy is properly accounted for. All 9 independent stiffness

components are almost never known. Even for a rock with TI symmetry all 5 independent components are usually not known. Due to lack of data, relations like equations (1) and (2) are therefore often used to estimate dynamic moduli for comparison with the static moduli given by Equations(3) and (4), however only in rare cases where the rock is nearly isotropic these equations may be used without introducing significant error.

5. **Strain amplitude.** Static moduli may be reduced as a result of non-elastic processes during monotonous loading over a finite range while the dynamic moduli remain unaffected. For instance, due to static friction, a closed crack or an uncemented grain contact may remain immobilized during the oscillating, low amplitude deformation associated with a passing elastic wave, whereas it may become mobilized as a result of static loading (Walsh 1965). This can be a major cause for differences between static and dynamic moduli. It is also the major reason why static-dynamic relations are highly sensitive to stress path and stress history.

It is the objective of this paper to give a review of the factors that may cause differences between static and dynamic moduli, and to show how they may be accounted for and possibly utilized. In the following chapters, each of these factors are discussed in detail, with examples of their importance and guidelines for how to eliminate or compensate for the effects experimentally. Suggested models for mathematical descriptions of the effects are also given. Finally, the last chapter gives some examples of how relations between static and dynamic data may be utilized, given that the various effects are properly accounted for.

## 2 STRAIN RATE

Static moduli are measures of the relationships between a change in stress and the corresponding deformation. Therefore, a finite strain rate may always be associated with static moduli.

The strain rate experienced by a rock volume due to a passing elastic wave is a periodic function, with amplitude ( $\dot{\varepsilon}_0$ ) related to the strain amplitude ( $\varepsilon_0$ ) as

$$\dot{\varepsilon}_0 = 2\pi f \varepsilon_0 \quad (5)$$

where  $f$  is the frequency. The strain amplitude of propagating elastic waves in rocks is typically limited to the range  $10^{-6} - 10^{-7}$  whereas the frequency may vary over many orders of magnitude. Hence, there is a close relationship between strain rate and frequency for such waves, as illustrated in Figure 1. By comparison, the strain rate induced during a typical rock mechanical laboratory test corresponds to the strain rate of an elastic wave with frequency about 1 Hz (Fjær, Stroisz and Holt 2013). Thus there is no fundamental difference in strain rate between static and dynamic moduli.

It is well established that dynamic stiffness may depend on frequency, in particular in shales (Spencer 1981; Duranti, Ewy and Hofmann 2005; Batzle, Han and Hofmann 2006; Bauer et al. 2016). This phenomenon is called dispersion. Different strain rates is therefore a possible cause for an observed difference between static and dynamic moduli; however, it depends on the actual static deformation rate and the frequency of the elastic waves applied. If the static and dynamic strain rates are equal, strain rate can be eliminated as a cause for difference between static and dynamic moduli. This is the case for dynamic moduli derived from seismic velocities in comparison with standard rock mechanical laboratory data. Laboratory measurements of seismic velocities is however rather demanding and usually implies that anisotropy effects cannot be eliminated simultaneously. This is a challenge for comparison of static and dynamic moduli under controlled conditions.

Dispersion may be modelled by a simple visco-elastic relation (Mavko, Mukerji and Dvorkin 1998):

$$M = \frac{\dot{s}_c^n M_0 + \dot{s}^n M_\infty}{\dot{s}_c^n + \dot{s}^n} \leftrightarrow \frac{f_c^n M_0 + f^n M_\infty}{f_c^n + f^n} \quad (6)$$

where  $M$  is the modulus at strain rate  $\dot{s}$  (or frequency  $f$ , for oscillatory deformations),  $M_0$  and  $M_\infty$  are the moduli corresponding to zero and infinite strain rate (or frequency), respectively, while  $\dot{s}_c$  is the transition rate (and  $f_c$  is the transition frequency). The exponent  $n$  is a positive number specifying the sharpness of the transition from low to high strain rates (or frequencies). Several other formulations also exist (for instance: Biot 1956b, 1956c; Murphy, Winkler and Kleinberg 1986; Holt, Fjær and Rzayev 2004; Gurevich et al. 2010), describing more or less the same behavior, but based on different physical explanations for the dispersion effect. If dispersion is the only effect that causes a difference between a static modulus and the corresponding dynamic modulus, the ratio between them is given as

$$\frac{M_{stat}}{M_{dyn}} = \frac{1 + \frac{M_\infty}{M_0} \left( \frac{\dot{s}}{\dot{s}_c} \right)^n}{1 + \left( \frac{\dot{s}}{\dot{s}_c} \right)^n} \frac{1 + \left( \frac{f}{f_c} \right)^n}{1 + \frac{M_\infty}{M_0} \left( \frac{f}{f_c} \right)^n} \quad (7)$$

where  $\dot{s}$  is the static strain rate and  $f$  is the dynamic frequency. Note that there is a relation between the transition strain rate and the transition frequency:

$$\dot{s}_c = af_c \quad (8)$$

The proportionality constant was estimated to  $a \sim 10^{-6} - 10^{-7}$  by Fjær, Stroisz and Holt (2013).

It is a common feature for all dispersion models that the rock is stiffer at higher frequencies, i.e.

$M_\infty > M_0$ . For dispersion caused by scattering, Biot flow or viscous shear relaxation,  $f_c \gg 10^2$  Hz (Mavko, Mukerji and Dvorkin 1998). This implies that  $\dot{s}_c \gg 10^{-5} - 10^{-4} \text{ s}^{-1}$  which is well above the typical range  $10^{-7} - 10^{-5} \text{ s}^{-1}$  for static strain rates in laboratory tests, hence  $\dot{s} \ll \dot{s}_c$ . According to equation (7) we therefore typically have  $M_{stat} < M_{dyn}$ . This is in accordance with most observations.

The differences induced by strain rate between dynamic moduli derived from different elastic waves (like ultrasonic versus seismic) may therefore be more significant than the difference induced by strain

rate between static and dynamic moduli. For dispersion caused by patchy saturation, and to some extent squirt flow,  $f_c \ll 10^2 \text{ Hz}$  is possible, giving  $\dot{s} > \dot{s}_c$ . According to equation (7) this opens up for the possibility that  $M_{stat} > M_{dyn}$ , as far as strain rate is concerned. This may happen if  $(\dot{s} / \dot{s}_c) > (f / f_c)$ , that is for relatively high static strain rate and relatively lower dynamic frequency compared to the dispersive transition.

Wave-induced fluid flow is often assumed to be the main origin of dispersion in sedimentary rocks (Batzle, Han and Hofmann 2006; Müller, Gurevich and Lebedev 2010; Bauer et al., 2016). The flow may occur on different length scales, from pore scale (Mavko and Nur 1979; O'Connell and Budiansky 1977), between patches of different saturation (White 1975) or global scale (Biot 1956a).

### 3 DRAINAGE CONDITIONS

Compression of a porous rock implies compression of the pore space. If the pores are fluid-filled, compression of the pore space will lead to an increase in the pore pressure, unless the pore fluid is allowed to escape. The increasing pore pressure will resist the compression of the rock and thus make the rock stiffer.

The impact of drainage conditions is well described by the Biot-Gassmann relations for an isotropic, linearly elastic, porous and permeable material (Gassmann 1951; Biot 1955, 1956a):

$$K = K_{fr} + K_f \frac{\left(1 - \frac{K_{fr}}{K_s}\right)^2}{\phi + \frac{K_f}{K_s} \left(1 - \phi - \frac{K_{fr}}{K_s}\right)} \quad (9)$$

$$G = G_{fr} \quad (10)$$

where  $K$  and  $G$  are the bulk and shear moduli when the rock is undrained,  $K_{fr}$  and  $G_{fr}$  are the corresponding moduli when the rock is drained,  $K_f$  and  $K_s$  are the bulk moduli of the fluid and the

solid component, and  $\phi$  is the porosity. The difference between drained and undrained moduli is illustrated in Figure 2. Given that dynamic moduli are always undrained, this also represents a potential difference between static and dynamic moduli if the static modulus is related to a drained deformation, which is often the case.

For anisotropic, non-linearly elastic materials with more than one solid phase, the relations are more complex and available descriptions correspondingly incomplete (Brown and Korringa 1975; Suarez-Rivera and Fjær 2013). Note also that equations (9) and (10) are based on the assumption that the entire pore space is connected.

To eliminate drainage conditions as a possible cause for a difference between static and dynamic moduli in a laboratory test, the static drainage conditions have to be similar to the dynamic conditions. If the rock is fully saturated, this implies that the static deformation has to be performed under undrained conditions. If the rock is dry or partly saturated with gas under atmospheric conditions, the low compressibility of the gas will prevent any significant fluctuations in pore pressure under undrained conditions, hence the drainage conditions are not important. Note that partial saturation may imply that liquid and gas are separated on a pore size scale, and that some pockets like thin cracks are fully liquid-filled. Due to restricted flow conditions this may result in spatial pore pressure fluctuations during dynamic loading. Such fluctuations give rise to dispersion effects (see above) however they do not induce any additional effect on the static-dynamic relationships.

#### 4 HETEROGENEITIES

Rock stiffness may vary a lot from one location to another, on all length scales. Even within the few centimeters covered by a core plug from a uniform formation there may be large variations in stiffness (Schei et al. 2000). Within a hundred meter range corresponding to the wavelength of a seismic wave even larger variations will normally occur, due to the presence of different rock types.

Such variations in stiffness have to be taken into account when comparing static and dynamic moduli. The effective stiffness of a heterogeneous rock volume is a combination of the stiffness, amount and

location of each homogeneous sub-volume. The dynamic stiffness derived from elastic waves that propagate through a portion of a rock volume is likely to differ from the effective stiffness of the entire volume. However, even when the volume involved by the static and dynamic measurements are the same, the dynamic stiffness may differ from the static stiffness. As an example, consider a stack of alternating stiff and soft layers. The effective stiffness corresponding to loading parallel to the layers depends on a combination of the individual stiffness of the layers and the relative amount of stiff and soft layers (Backus 1962), and falls somewhere between the stiffness of the stiffest and softest layer. For elastic waves travelling in the same direction, at least a portion of the wave front will follow the stiffest layers, and hence the dynamic stiffness based on the velocities of the first arrivals may be nearly the same as if the entire volume consisted of the stiffest material.

Note that the effective stiffness for an elastic wave depends on the wavelength relative to the size of the heterogeneities. This effect was nicely demonstrated experimentally by Marion and Coudin (1992) and theoretically by Hovem (1995) for waves travelling normal to the layers in a layered material. If the frequency is sufficiently low such that the wavelength is much larger than the layer thickness, the wave will sense the effective stiffness of the layered material just like a static loading, and the dynamic and static stiffness will be equal:

$$M_{stat} = M_{dyn} = \left\langle \frac{1}{M} \right\rangle^{-1} \quad (11)$$

$\langle x \rangle$  represents the average of the parameter  $x$ , weighted by the volumetric proportion of each layer (also known as "Backus average"). If the frequency is sufficiently high so that the wavelength is much smaller than the layer thickness, the wave will sense each layer individually and the total traveltimes will be the sum of the traveltimes through all layers, giving a dynamic stiffness that is generally higher than the static stiffness:

$$M_{dyn} = \rho \left\langle \sqrt{\frac{\rho}{M}} \right\rangle^{-2} \geq \left\langle \frac{1}{M} \right\rangle^{-1} = M_{stat} \quad (12)$$

where  $\rho$  is density. This implies that heterogeneities in density may also have an impact on the relations between static and dynamic moduli, even if the stiffness is uniform.

The considerations above were based on the assumption that the static loading includes the entire rock volume. This is not always the case, of course. For instance, the static stiffness derived from a core plug tested in the laboratory only represents the stiffness of a small fraction of the volume covered within the wavelength of a seismic wave. Thus, a comparison of the static stiffness measured on the plug to the dynamic stiffness derived from the seismic velocity may well show that the static stiffness is higher. This may even be the case if the static stiffness is estimated as the average over stiffness measured on a representative selection of core plugs from the entire volume covered by the seismic wavelength, since simple averaging may not be the correct way to upscale stiffness (cf. equation (11)). This depends on the orientation of the load and the distribution of the heterogeneities however, as described by Backus (1962).

For a reasonably homogeneous core plug subject to static and dynamic measurements in the laboratory, rock volume effects are not likely to have a significant impact on the ratio between static and dynamic stiffness.

## 5 ANISOTROPY

Anisotropy is a potential pitfall while comparing static and dynamic moduli. It may be tempting to estimate for instance dynamic bulk modulus based on equation (1), or dynamic Young's modulus based on equation (2), ignoring anisotropy. However, this simplification may introduce large errors if the rock is anisotropic, which is usually the case for sedimentary rocks. When sufficient data is available, an anisotropic dynamic stiffness tensor may be established by combining wave velocities measured in different directions. It is rarely possible to establish a complete tensor this way, even for a rock that possesses TI symmetry, due to lack of data. However, combining the available data with reasonable assumptions such as elliptical anisotropy (Helbig 1983)

$$C_{13} = \sqrt{(C_{11} - C_{44})(C_{33} - C_{44})} - C_{44} \quad (13)$$

may improve the estimates significantly compared to the isotropic assumption.

Given the complexity of static-dynamic relations, it is not obvious that static and dynamic anisotropy are uniquely related. Holt et al. (2015) compared static and dynamic anisotropy for a set of shale cores, and found that scaling of the dynamic stiffness (derived from ultrasonic velocities) with a suitable constant reproduced fairly well the static stiffness obtained from stress cycles, similar to the results found by Miller, Plumb and Boitnott (2013). On the other hand, the difference between this cycling static stiffness and the static stiffness obtained during initial loading (further discussed in the next section) was in terms of anisotropy reproduced by a constant shift rather than scaling. Thus, comparing dynamic stiffness derived from ultrasonic velocities with static stiffness during initial loading produces a static-dynamic anisotropy relation that cannot be reproduced by pure scaling nor by pure shift. This is not surprising since such a comparison involves at least two mechanisms, dispersion and non-elastic deformation, that have different anisotropic properties.

In a laboratory experiment, anisotropy may easily be eliminated as a source of error if the test is suitably designed, as illustrated in Figure 3. The sample is loaded axially while lateral deformation is restricted (i.e.  $\Delta\varepsilon_r = 0$ ). The static modulus  $H_{stat}$  is found as the ratio between the axial stress increment  $\Delta\sigma_z$  and the corresponding axial strain increment  $\Delta\varepsilon_z$ :

$$H_{stat} = \left. \frac{\Delta\sigma_z}{\Delta\varepsilon_z} \right|_{\Delta\varepsilon_r=0} \quad (14)$$

The P-wave velocity  $V_{pz}$  is derived from the traveltime between the two transducers aligned along the sample axis, and the dynamic modulus  $H_{dyn}$ , also known as the plane wave modulus, is given as

$$H_{dyn} = \rho V_{pz}^2 \quad (15)$$

Under these conditions,  $H_{stat}$  and  $H_{dyn}$  represent the same stiffness coefficient ( $C_{33}$ ) and can be related without any further concern about anisotropy in this case.

This implies that the velocity of a vertically propagating P-wave may be used to estimate the dynamic stiffness corresponding to vertical compaction under zero lateral deformation, a condition that is often assumed to be valid for a depleting reservoir. Note however that the stacking velocities produced by seismic processing may appear as vertical velocities, even though they are derived from waves propagating at a significant inclination and hence are affected by anisotropy.

## 6 STRAIN AMPLITUDE

Difference in strain amplitude is considered to be a major cause for the differences between static and dynamic moduli (Walsh 1965; Yale and Jamieson 1994; Tutuncu et al. 1998; Fjær 1999). In a heterogeneous material like a sedimentary rock, a stress increment not only induces an elastic, recoverable deformation, it also tends to involve non-elastic processes, such as slip and sliding of internal surfaces. These processes induce additional, non-elastic strain components that do not alter the strain energy in the material. Stiffness, defined as the stress increment divided by the total strain increment, is therefore reduced as a result of such non-elastic processes. These non-elastic processes and the corresponding non-elastic strain components depend strongly on the stress path and the stress history. For simplicity, we shall here assume that these processes can be illustrated by activation of sliding cracks, and crushing of asperities at grain contacts (Stroisz and Fjær 2012). Clearly, this simplification implies that we allow for a rather wide definition of cracks and grain contacts. As explained by Walsh (1965) (see also Moss and Gupta 1982; David et al. 2012), a closed crack will slide as the shear stress across the cracks surface exceeds the static friction, but will remain locked as long as the shear stress does not reach this limit. This implies that a negative stress increment may also activate crack sliding, but only when the increment is sufficiently large so that the shear stress across the crack exceeds the static friction in the opposite direction. Upon reloading, the static friction will again prevent sliding until the shear stress is sufficiently large. The small, oscillating shear stress

amplitude induced by an elastic wave is not sufficient to activate a significant amount of such sliding cracks, hence the sliding processes mainly affect the static moduli. Walsh used this argument to establish a relation between the static and dynamic Young's moduli ( $E_{stat}$  and  $E_{dyn}$ , respectively):

$$E_{stat} = \frac{E_{dyn}}{1 + w} \quad (16)$$

Here, the crack contribution has been assembled in the parameter  $w$  which is proportional to the density of sliding cracks (the exact expression for  $w$  depends on the stress geometry, as shown by Walsh). In a stress path as illustrated in Figure 4 we may expect the following development in accordance with the arguments above: During initial loading, an increasing number of sliding cracks will be activated, hence  $w$  will have a finite and growing value. When loading is reversed, all sliding cracks will be locked initially and gradually become activated as unloading proceeds, hence  $w$  will drop to zero initially and slowly build up again as the unloading path is increasing. When reloading is initiated, all sliding cracks will be locked initially and gradually become activated as reloading proceeds, hence  $w$  will again drop to zero initially and slowly build up as the reloading path is increasing. When the stress exceeds its previous peak value, potential sliding cracks that were close to become activated prior to the start of the unloading cycle will now be activated, as they would have been at the same stress level if the unloading cycle had been skipped. Hence,  $w$  will continue along its initial loading path. According to equation (16), this produces a relationship between the static and dynamic moduli very similar to the observations shown in Figure 4. Since  $w$  is a non-negative number, equation (16) states that  $E_{stat} \leq E_{dyn}$ . This is probably the main reason why static stiffness is usually found to be smaller than dynamic stiffness.

This example clearly demonstrates that the relationship between static and dynamic moduli depends strongly on the stress path and the stress history. The other non-elastic process mentioned above, crushing of asperities at grain contacts, has a similar effect on this relationship: The crushing process will be active, inducing a non-elastic strain component, during initial loading. During unloading and

reloading, the process will be more or less absent, while it will return to its initial level when the stress increases beyond its historical peak value.

Fjær (1999) presented a model describing how the non-elastic processes control the relations between static and dynamic moduli during initial loading on dry sandstone in triaxial test conditions. According to this model, the static and dynamic bulk moduli ( $K_{stat}$  and  $K_{dyn}$ , respectively) are related as

$$K_{stat} = \frac{K_{dyn}}{1 + (P_z + 2P_r)K_{dyn}} \quad (17)$$

while the static and dynamic Young's moduli are related as

$$E_{stat} = \frac{E_{dyn}}{1 + P_z E_{dyn}} (1 - F) \quad (18)$$

The non-elastic processes are described by the parameters  $P_r$ ,  $P_z$  and  $F$ . It was found that

$$P_i = \frac{\varepsilon_g}{\sigma_i + T} \quad (19)$$

The parameter  $F$  depends on stress and strain as

$$F = A \frac{\varepsilon_z - \varepsilon_r - \varepsilon_0}{\sqrt{\sigma_z + \sigma_r + S}} \quad (20)$$

where  $\varepsilon_z$  and  $\varepsilon_r$  are the axial and radial strain, respectively, and  $\varepsilon_0 = \varepsilon_z - \varepsilon_r$  at the start of the triaxial phase.  $\varepsilon_g$ ,  $T$ ,  $A$  and  $S$  are constants. While  $P_r$  and  $P_z$  are mostly associated with crushing of grain contacts,  $F$  is associated with sliding cracks. Note that for  $P_z = 0$  (negligible crushing at grain contacts), equations (18) and (16) coincide if  $F \leftrightarrow w$  and  $F \ll 1$ . Unlike equation (16) however, equation (18) implicitly accounts for interactions between the sliding cracks, hence the expression may be applied for concentrations of sliding cracks even as high as for  $F = 1$ , where  $E_{stat} = 0$ . The model may therefore be used to describe the relations between the static and dynamic

moduli during the entire triaxial test, including the peak stress point. The predictions of this model are supported by experimental data and by discrete particle simulations (Li and Fjær 2012). The model was developed for sandstone with limited clay content. Later studies (Holt et al. 2012) have indicated that the model may also be applicable for shale.

Based on the arguments of Walsh (1965), we may draw the conclusion that there will be a finite stress range at the start of an unloading path where the rock is fully elastic and the static and dynamic moduli are equal, since the shear stress across the cracks needs to be reversed and grow up to the static friction level in the opposite direction before sliding is initiated. Such a fully elastic range appears to be much smaller than any practical static loading path however. It is seen that the deviation between static and dynamic moduli associated with strain amplitude starts to grow immediately as the unloading path exceeds about  $5 \cdot 10^{-6}$ , i.e. the typical amplitude of an elastic wave (Martin and Haupt 1994; Tutuncu et al. 1998; Lozovyi et al. 2017). Grain pack models (Duffy and Mindlin 1957; Stoll 1989; Nihei et al. 2000) may offer an explanation for this. In this context, we may consider the contact area between two grains as a closed crack. When two spherical grains are pressed together by a normal force and then subjected to a shear load, there will be a region at the edge of the contact area where the shear stress is high while the normal stress is vanishing. Since the static friction is proportional to the normal stress, there will – theoretically – be areas where even the smallest alteration of the shear stress is sufficient to overcome the static friction and hence activate a non-elastic process. Clearly, the level of such activity will increase as the unloading continues.

Based on observations, Fjær et al. (2011) concluded that the "non-elastic compliance", defined as the difference between corresponding static and dynamic compliances, appears to increase linearly with decreasing stress during unloading. For instance, the non-elastic compliance associated with the plane wave modulus  $H$  is a linear function of stress during unloading (Figure 5):

$$S_H \equiv \frac{1}{H_{stat}} - \frac{1}{H_{dyn}} = a(\sigma_z^* - \sigma_z) + b \quad (21)$$

$\sigma_z^*$  is the axial stress at the start of the unloading sequence, and  $a$  and  $b$  are constants. The linear relationship may extend for several tens of MPa below  $\sigma_z^*$  (Stroisz 2013). Lozovyi et al. (2017) on the other hand observed the same linear relationship for strain amplitudes as low as  $5 \cdot 10^{-6}$ , i.e. within the range of elastic waves. Thus, the constant  $b$  represents the difference between  $H_{stat}$  and  $H_{dyn}$  for all other causes than the strain amplitude, at  $\sigma_z = \sigma_z^*$ .

According to equation (21), the difference between static and dynamic moduli, as measured during unloading-reloading cycles, will increase with increasing amplitude of the cycles. This is in accordance with observations (Plona and Cook 1995). The constant  $a$  is found to decrease with increasing  $\sigma_z^*$  (Fjær, Holt and Stroisz 2015), in qualitative agreement with the relationship

$$a = - \left. \frac{dS_H}{d\sigma_z} \right|_{\sigma_z = \sigma_z^*} \sim (\sigma_z^*)^{-4/3} \quad (22)$$

which can be derived from the grain pack model (Stoll 1989; Nihei et al. 2000). This model does not predict a linear relationship as expressed by equation (21) however.

An important conclusion from these observations is that the ratio between corresponding static and dynamic moduli is a function of stress state as well as stress history. Thus, presenting this ratio as a simple number only makes sense if it is linked to a specific stress state and stress history.

## 7 COMBINED EFFECTS

The previous chapters describe how individual mechanisms and effects may induce differences between static and dynamic moduli. Quite often, two or more of these effects may be in play together. Analysis of such a situation is generally complicated, as the various effects can be coupled. However, as a start, it may be helpful to approach the problem step by step, adding one effect at the time while keeping track of the type of deformation reached in each step.

Consider as an example a situation where a fully saturated rock sample undergoes drained hydrostatic loading beyond the previous peak stress level. The static bulk modulus is measured as the slope of the stress-strain curve and the dynamic bulk modulus is derived from ultrasonic waves. Starting with the dynamic modulus  $K_{dyn}$ , this modulus represents an undrained deformation with infinitely small strain amplitude and strain rate given by the dynamic frequency  $f$ . Equation (7) gives us the bulk modulus  $K_1$  corresponding to the static strain rate  $\dot{s}$  (still undrained, and with infinitely small strain amplitude):

$$K_1 = \frac{1 + \frac{K_\infty}{K_0} \left( \frac{\dot{s}}{\dot{s}_c} \right)^n}{1 + \left( \frac{\dot{s}}{\dot{s}_c} \right)^n} \frac{1 + \left( \frac{f}{f_c} \right)^n}{1 + \frac{K_\infty}{K_0} \left( \frac{f}{f_c} \right)^n} K_{dyn} \quad (23)$$

where  $K_0$  and  $K_\infty$  represent undrained bulk modulus at zero and infinite strain rate, respectively, in the limit of zero strain amplitude. Further, equation (17) gives us the bulk modulus  $K_2$  corresponding to the static strain amplitude during initial loading beyond the previous peak stress level (undrained, with strain rate  $\dot{s}$ ):

$$K_2 = \frac{K_1}{1 + (P_z + 2P_r) K_1} \quad (24)$$

Finally, the drained bulk modulus corresponding to the static strain rate and strain amplitude during initial loading beyond the previous peak stress,  $K_{stat}$ , can be derived by the help of equation (9):

$$K_{stat} + K_f \frac{\left( 1 - \frac{K_{stat}}{K_s} \right)^2}{\phi + \frac{K_f}{K_s} \left( 1 - \phi - \frac{K_{stat}}{K_s} \right)} = K_2 \quad (25)$$

If the rock is heterogeneous, for instance layered as discussed in chapter 4, each layer can usually be analyzed individually with respect to strain rate, strain amplitude and saturation. The properties of

each layer may then be combined, in accordance with layer thickness relative to wavelength and static load, in order to account for the heterogeneities. Such a step by step approach may not always be possible however, as the different mechanisms can be coupled.

Anisotropy is generally a complicating element, where the main challenge is to ensure that corresponding static and dynamic moduli can be compared, as described in chapter 5. However, each mechanism that can cause a difference between static and dynamic moduli may introduce a different symmetry, and this needs to be accounted for in each step of the analysis. Note also that anisotropy is always due to heterogeneities on a scale smaller than the scale where it is observed. In a situation like the example given in chapter 4 (equation (12)), the heterogeneities not only introduce a difference in magnitude between static and dynamic moduli, but they also induce an additional element of anisotropy which is different for the two types of moduli, since the static scale is larger than the heterogeneities while the dynamic scale is smaller.

## 8 APPLICATIONS

Knowledge about the relations between static and dynamic moduli provide some useful tools for analysis and prediction of rock behavior. A couple of examples are given here.

### 8.1 Dispersion

Interpretation of time lapse seismic data can be challenging, but the value of such data can be largely enhanced if the stress dependency of the seismic velocities is known. Laboratory measurements on core plugs may reveal this stress dependency. However, measurements at ultrasonic frequencies have limited value unless the dispersion in the range from seismic to ultrasonic frequencies is known.

Valuable information may be obtained from measurements of dynamic Young's modulus and Poisson's ratio at seismic frequencies (Spencer 1981; Duranti, Ewy and Hofmann 2005; Batzle, Han and Hofmann 2006; Szewczyk, Bauer and Holt 2016), however such measurements are complicated

and require special equipment, and has only been reported by a few laboratories. Anisotropy is also a challenge for the interpretation.

The "static" strain rate of a standard laboratory test is typically in the order of 1 Hz (Fjær, Stroisz and Holt 2013). This offers a possibility for estimation of dispersion between seismic and ultrasonic frequencies, by comparing static and dynamic moduli. Such a utilization of the test data requires however, that strain rate can be isolated as the only cause for the difference between static and dynamic moduli. The main obstacle for achieving this is the strain amplitude, since standard measurements of the static modulus (equation (14)) require a strain amplitude that is orders of magnitude larger than the amplitude of the elastic wave. However, the strain amplitude effect can be eliminated as follows: By measuring static and dynamic moduli over a suitable stress interval during unloading, and matching the data to equation (21), it is possible to identify the parameter  $b$  by extrapolating the straight line to the start of the unloading path. This procedure allows us to eliminate the strain amplitude effect, as the parameter  $b$  represents the difference between static and dynamic moduli at the start of the unloading sequence, for all other causes than strain amplitude. If impact from saturation, heterogeneities and anisotropy have also been eliminated, as discussed above, the static modulus at the start of the unloading sequence and the dynamic modulus at seismic frequencies are equal (within reasonable limits of accuracy). Thus, the seismic velocity  $V_{P,seis}$  can be derived from the ultrasonic velocity  $V_{P,ultra}$  as (Fjær, Stroisz and Holt 2013):

$$V_{P,seis} = \frac{V_{P,ultra}}{\sqrt{1 + \rho b V_{P,ultra}^2}} \quad (26)$$

This "zero strain extrapolation" method may be used to estimate dispersion at specific points along the stress path, using only standard rock mechanical test equipment. Bauer et al. (2016) demonstrated that the method yields results in good agreement with low frequency measurements of dynamic Young's modulus.

## 8.2 Strength and static stiffness from dynamic measurements

Several field operations, like for instance sand prediction, hydraulic fracturing, evaluation of borehole stability or reservoir compaction, require estimates of strength and stiffness in areas where only logs or seismic data are available. A quantitative model describing the relations between static and dynamic moduli has the potential to bridge this gap between available and requested information.

Numerous empirical models have been introduced for this purpose (for instance: King 1983, Eissa and Kazi 1988, Jizba and Nur 1990, Yale and Jamieson 1994, Lacy 1997, Olsen, Christensen and Fabricius 2008, Zoveidavianpoor 2017). Such models may be useful for a specific purpose within a given area, however they may also be misleading if they are applied for other purposes or in other areas. A major drawback with such models is that they state that the ratio between a static and the corresponding dynamic modulus is a single number. This is not only misleading, it also suppresses useful information. Whereas for instance the dynamic Young's modulus may have a fairly low sensitivity to stress state and stress path, the static modulus can vary a lot – possibly in the entire range between zero and the dynamic value (Fjær 2009). Thus, providing a single estimate of a static modulus on the basis of an empirical correlation with the dynamic modulus is not enough; also, the context in which the static modulus is going to be applied must be taken into account, as the relevant value can vary so much.

Application of equations (17) - (20), which are covering initial loading in a triaxial test geometry, is an example of a more detailed and thorough approach. In combination with a model for stress dependent wave velocities, these equations make a constitutive model for rock mechanical behavior during an entire triaxial test. A tool for estimation of strength and stiffness based on wireline logs has been based on this model (Raaen et al. 1996; Woehrl et al. 2010). The tool works as follows: log data from a given position is used to calibrate the model (i.e. values for the model parameters  $A$ ,  $\varepsilon_g$  etc. are estimated on the basis of the log data, using empirical correlations). The calibrated model is used to simulate a standard rock mechanical test on a fictitious core sample from this position, yielding both strength and stiffness in the same way as a real test. As this test is only a numerical simulation, it can be repeated several times with different confining pressures, thus also providing an estimate for the friction angle.

## 9 CONCLUSIONS

Static and dynamic moduli of rocks are generally different, for a number of potential reasons: different strain rates, different drainage conditions, different strain amplitudes, and spatial variations in rock properties. Relations between the static and dynamic moduli are complex, and meaningful comparison requires precise description of several conditions, in particular saturation and drainage conditions, dynamic frequency and static strain rate, and stress state and stress history. In addition, the rock volumes involved must be representative, and anisotropy must be properly accounted for.

In order to study each of the various mechanisms causing differences between static and dynamic moduli, the other effects need to be eliminated through careful design and execution of tests.

Elimination of the strain amplitude effect is particularly challenging, since measurements of static stiffness usually requires strain amplitudes several orders of magnitude larger than the dynamic amplitudes. However, utilization of the linear relationship between non-elastic compliance and stress during unloading makes it possible to eliminate also this effect, by extrapolation to zero strain amplitude.

Mathematical models, allowing for quantitative description with reasonable precision, are available for each of the mechanisms. These models may be useful for analysis of rock behavior. Given proper calibration, they may also be used for prediction of rock behavior, and for estimation of static properties based on dynamic data, which can be particularly useful in field situations where only dynamic data are available. Conversely, static measurements may be used to estimate seismic velocities, which can be useful for evaluation of dispersion in the range between seismic and ultrasonic frequencies.

### **Acknowledgement**

This work was supported financially by the SINTEF project "Shale Rock Physics: Improved seismic monitoring for increased recovery", sponsored by The Research Council of Norway (Grant no. 234074/E30), Aker BP, DONG Energy, Engie, Maersk and Total.

## References

- Backus, G.E. 1962. Long-wave elastic anisotropy produced by horizontal layering. *Journal of Geophysical Research* **67**, 4427–4440.
- Batzle, M. L., Han, D.-H. and Hofmann, R. 2006. Fluid mobility and frequency-dependent seismic velocity - Direct measurements. *Geophysics* **71**, N1–N9.
- Bauer, A., Bhuiyan, M.H., Fjær, E., Holt, R.M., Lozovyi, S., Pohl, M. and Szewczyk, D. 2016. Frequency-dependent wave velocities in sediments and sedimentary rocks: Laboratory measurements and evidences. *The Leading Edge* **35**, 490–494.
- Biot, M.A. 1955. Theory of elasticity and consolidation for a porous anisotropic solid. *Journal of Applied Physics* **26**, 182–185.
- Biot, M.A. 1956. General solutions of the equations of elasticity and consolidation for a porous material. *Journal of Applied Mechanics* **23**, 91–96.
- Biot, M.A. 1956a. Theory of propagation of elastic waves in a fluid-saturated porous solid. I. Low-frequency range. *Journal of the Acoustic Society of America* **28**, 168–178.
- Biot, M.A. 1956b. Theory of propagation of elastic waves in a fluid-saturated porous solid. II. Higher frequency range. *Journal of the Acoustic Society of America* **28**, 179–191.
- Brown R.J.S. and Korrinda, J. 1975. On the dependence of the elastic properties of a porous rock on the compressibility of the pore fluid. *Geophysics* **40**, 608–616.
- Cheng, C. H. and Johnston, D.H. 1981. Dynamic and static moduli. *Geophysical Research Letters* **8**, 39–42.
- David, E.C., Brantut, N., Schubnel, A. and Zimmerman, R.W. 2012. Sliding crack model for nonlinearity and hysteresis in the uniaxial stress–strain curve of rock. *International Journal of Rock Mechanics & Mining Sciences* **52**, 9-17.
- Duffy, J. and Mindlin, R. D. 1957. Stress-strain relations and vibrations of a granular medium. *Journal of Applied Mechanics* **24**, 585-593.

- Duranti, L., Ewy, R. and Hofmann, R. 2005. Dispersive and attenuative nature of shales: Multiscale and multifrequency observations. *75th International SEG Meeting*, Houston, USA, Expanded Abstracts 1577–1580.
- Eissa, E.A. and Kazi, A. 1988. Relation between static and dynamic Young's moduli of rocks. *International Journal of Rock Mineral Science and Geomechanical Abstracts* **25**, 479–482.
- Fjær, E. 1999. Static and dynamic moduli of weak sandstones. In: *Rock mechanics for industry* (eds. B. Amadei *et al*) pp. 675–681. Balkema.
- Fjær, E. 2009. Static and dynamic moduli of a weak sandstone. *Geophysics* **74**, WA103-WA112.
- Fjær, E., Holt, R.M., Nes, O.-M. and Stenebråten, J.F. 2011. The transition from elastic to non-elastic behavior. *45th US Rock Mechanics/Geomechanics Symposium*. San Francisco, USA, ARMA 11-389.
- Fjær, E., Stroisz, A.M. and Holt, R.M. 2013. Elastic dispersion derived from a combination of static and dynamic measurements. *Rock Mechanics and Rock Engineering* **46**, 611–618.
- Fjær, E., Holt, R.M. and Stroisz, A.M. 2015. Relating static stiffness to ultrasonic, sonic and seismic velocities. 3rd International Workshop on Rock Physics, Perth, Australia. Expanded Abstract.
- Gassmann, F. 1951. Über die Elastizität poröser Medien. *Vierteljahrsschrift der Naturforschenden Gesellschaft in Zürich* **96**, 1–23.
- Gurevich, B., Makarynska, D., de Paula, O.B. and Pervukhina, M. 2010. A simple model for squirt-flow dispersion and attenuation in fluid-saturated granular rocks. *Geophysics* **75**, P.N109-N120.
- Helbig, K. 1983. Elliptical anisotropy – Its significance and meaning. *Geophysics* **48**, 825-832.
- Holt, R.M., Fjær, E. and Rzayev, E. 2004. P- and S-wave velocities in shales: Experiments and a model. *6th North America Rock Mechanics Symposium*. Houston, USA, ARMA/NARMS 04-543.
- Holt, R.M., Nes, O.-M., Stenebråten, J.F. and Fjær, E. 2012. Static vs dynamic behavior of shale. *46th US Rock Mechanics/Geomechanics Symposium*. Chicago, USA. ARMA 12-542.

- Holt, R.M., Bauer, A., Fjær, E., Stenebråten, J.F., Szewczyk, D. and Horsrud, P. 2015. Relating Static and Dynamic Mechanical Anisotropies of Shale. *49th US Rock Mechanics/Geomechanics Symposium*. San Francisco, USA. ARMA 15-484
- Hovem, J.M. 1995. Acoustic waves in finely layered media. *Geophysics* **60**, 1217–1221.
- Jizba, D. and Nur, A. 1990. Static and dynamic moduli of tight gas sandstones and their relation to formation properties. *31st Annual Logging Symposium*, Society of Professional Well Log Analysts, Paper BB.
- King, M. S. 1970. Static and dynamic elastic moduli of rocks under pressure. *11th U. S. Symposium on Rock Mechanics*, Berkeley, USA. ARMA Proceedings, 329–351.
- King, M.S. 1983. Static and dynamic elastic properties of rocks from the Canadian Shield. *International Journal of Rock Mineral Science and Geomechanical Abstracts* **20**, 237–241.
- Lacy, L.L. 1997. Dynamic rock mechanics testing for optimized fracture design. *SPE Annual Technical Conference and Exhibition*, San Antonio, USA. SPE 38716.
- Ledbetter, H. 1993. Dynamic vs. static Young's moduli: a case study. *Materials Science and Engineering* **A165**, L9-L10
- Li, L. and Fjær, E. 2012. Modeling of stress-dependent static and dynamic moduli of weak sandstones. *Journal of Geophysical Research – Solid Earth* **117**, B05206.
- Lozovyi, S., Sirevaag T., Szewczyk, D., Bauer, A. and Fjær, E. 2017. Non-elastic effects in static and dynamic rock stiffness. *51st US Rock Mechanics / Geomechanics Symposium*. San Francisco, USA. ARMA 17-293.
- Marion, D. P. and Coudin, P. 1992. From ray to effective medium theories in stratified media: An experimental study. *62nd International SEG Meeting*, New Orleans, USA. Expanded Abstracts, 1341–1343.
- Martin, R. J. III and Haupt, R.W. 1994. Static and dynamic elastic moduli on granite: The effect of strain amplitude. In: *Rock mechanics* (eds. P. P. Nelson and S. E. Lauback) pp. 473–480. Balkema.

- Mavko, G. and Nur, A. 1979. Wave attenuation in partially saturated rocks. *Geophysics* **44**, 161–178.
- Mavko, G. Mukerji, T. and Dvorkin, J. 1998. *The rock physics handbook*. Cambridge University Press.
- Miller, D., Plumb, R. and Boitnott, G. 2013. Compressive strength and elastic properties of a transversely isotropic calcareous mudstone. *Geophysical Prospecting* **61**, 315-328.
- Moss, W.C. and Gupta, Y.M. 1982. A constitutive model describing dilatancy and cracking in brittle rocks. *Journal of Geophysical Research* **87**, 2985-2998.
- Murphy III, W.F., Winkler, K.W. and Kleinberg, R.L. 1986. Acoustic relaxation in sedimentary rocks: Dependence on grain contacts and fluid saturation. *Geophysics* **51**, 757-766.
- Murphy, W., Reischer, A. and Hsu, K. 1993. Modulus decomposition of compressional and shear velocities in sand bodies. *Geophysics* **58**, 227–239.
- Müller, T. M., Gurevich, B. and Lebedev, M. 2010. Seismic wave attenuation and dispersion resulting from wave-induced flow in porous rocks - A review. *Geophysics* **75**, 75A147–75A164.
- Nihei, K.T., Hilbert Jr, L.B., Cook, N.G.W., Nakagawa, S. and Myer, L.R. 2000. Friction effects on the volumetric strain of sandstone. *International Journal of Rock Mechanics and Mining Sciences* **37**, 121-132.
- O'Connell, R.J. and Budiansky, B. 1977. Viscoelastic properties of fluid-saturated cracked solids. *Journal of Geophysical Research* **82**, 5719-5735.
- Olsen, O., Christensen, H.F. and Fabricius, I.L. 2008. Static and dynamic Young's moduli of chalk from the North Sea. *Geophysics* **73**, E41-E50.
- Plona, T.J. and Cook, J.M. 1995. Effects of stress cycles on static and dynamic Young's moduli in Castlegate sandstone. In: *Rock mechanics: Proceedings of the 35th U.S. symposium* (eds. J.J.K. Daemen, and R.A. Schultz) pp. 155–160. Balkema.
- Raaen, A. M., Hovem, K. A., Jøranson, H. and Fjær, E. 1996. FORMEL: A step forward in strength logging: *SPE ATCE 1996*. Denver, USA. SPE 36533.

- Schei, G., Fjær, E., Detournay, E., Kenter, C. J., Fuh, G. F. and Zausa, F. 2000. The Scratch Test: An Attractive Technique for Determining Strength and Elastic Properties of Sedimentary Rocks. *SPE ATCE 2000*. Dallas, USA. SPE 63255.
- Simmons, G. and Brace, W.F. 1965. Comparison of static and dynamic measurements of compressibility of rocks. *Journal of Geophysical Research* **70**, 5649–5656.
- Spencer Jr., J. W. 1981. Stress relaxation at low frequencies in fluid saturated rocks: Attenuation and modulus dispersion. *Journal of Geophysical Research* **86**, B3, 1803–1812.
- Stoll, R.D. 1989. Stress-induced anisotropy in sediment acoustics. *Journal of the Acoustic Society of America* **85**. 702-708.
- Stroisz, A.M. and Fjær, E. 2012. Tracing causes for the stress sensitivity of elastic wave velocities in dry Castlegate sandstone. *Geophysical Journal International* **192**, 137-147.
- Stroisz, A.M. 2013. Nonlinear elastic waves for estimation of rock properties. PhD Theses. Norwegian University of Science and Technology.
- Suarez-Rivera, R. and Fjær, E. 2013. Evaluating the poroelastic effect on anisotropic, organic-rich, mudstone systems. *Rock Mechanics and Rock Engineering* **46**, 569–580.
- Szewczyk, D., Bauer, A. and Holt, R.M. 2016. A new laboratory apparatus for the measurement of seismic dispersion under deviatoric stress conditions. *Geophysical Prospecting* **64**, 789-798.
- Tutuncu, A.N., Podio, A.L., Gregory, A.R. and Sharma, M.M. 1998. Nonlinear viscoelastic behavior of sedimentary rocks, Part I: Effect of frequency and strain amplitude. *Geophysics*, **63**, 184-194.
- Walsh, J. B. 1965. The effect of cracks on the uniaxial compression of rocks. *Journal of Geophysical Research* **70**, 399–411.
- White, J. E. 1975. Computed seismic speeds and attenuation in rocks with partial gas saturation: *Geophysics* **40**, 224–232.

Woehrl, B., Wessling, S., Bartetzko, A., Pei, J. and Renner, J. 2010. Comparison of Methods to Derive Rock Mechanical Properties from Formation Evaluation Logs. *44th U.S. Rock Mechanics Symposium and 5th U.S.-Canada Rock Mechanics Symposium*. Salt Lake City, USA. ARMA 10-167.

Yale, D.P. and Jamieson Jr, W.H. 1994. Static and dynamic mechanical properties of carbonates. In: *Rock mechanics* (eds. P. P. Nelson and S. E. Lauback) pp. 463–471. Balkema.

Zoveidavianpoor, M. 2017. An integrated approach in determination of elastic rock properties from well log data in a heterogeneous carbonate reservoir. *Journal of Petroleum Science and Engineering* **153**, 314-324.

## Figure captions

- Figure 1** Typical frequencies and strain rates for common wave types. The arrow indicate the strain rate of a typical rock mechanical laboratory test.
- Figure 2** Ratio between corresponding moduli for drained and undrained rock, according to the Biot-Gassmann theory. The frame moduli are assumed to depend on porosity according to the empirical model of Murphy, Reischer and Hsu (1993) for sandstone.
- Figure 3** Test conditions allowing to compare directly static and dynamic modulus.
- Figure 4** Ratio between static and dynamic uniaxial compaction modulus along a loading-unloading-reloading stress path.
- Figure 5** Non-elastic compliance  $S_H$  versus axial stress  $\sigma_z$ , from an unloading sequence starting at  $\sigma_z^*$  in a tests on a dry sandstone.

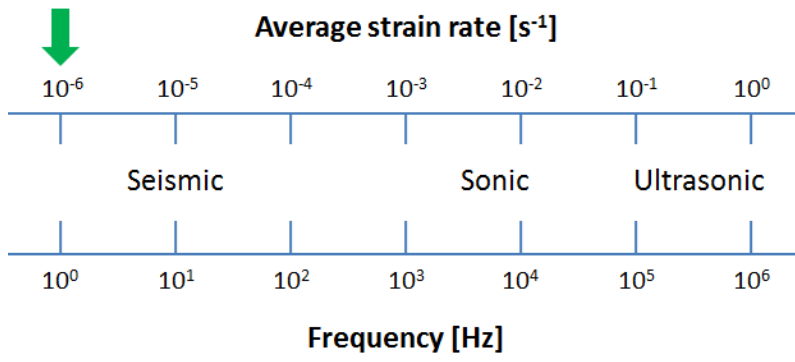


Figure 1

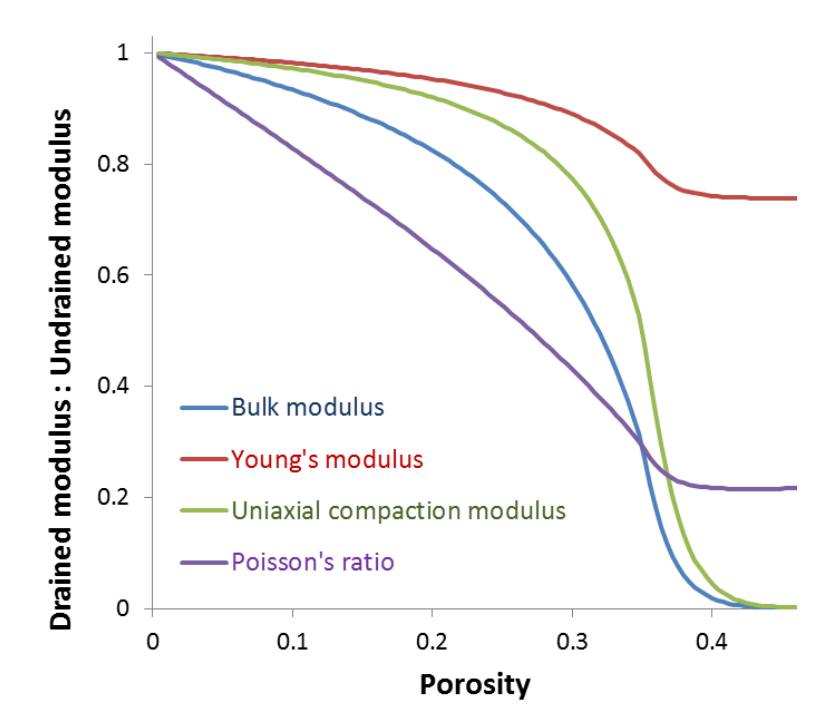


Figure 2

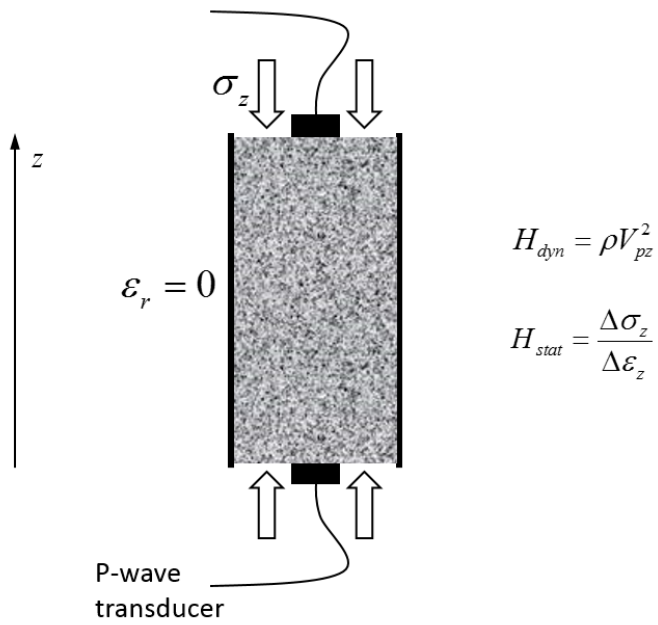


Figure 3

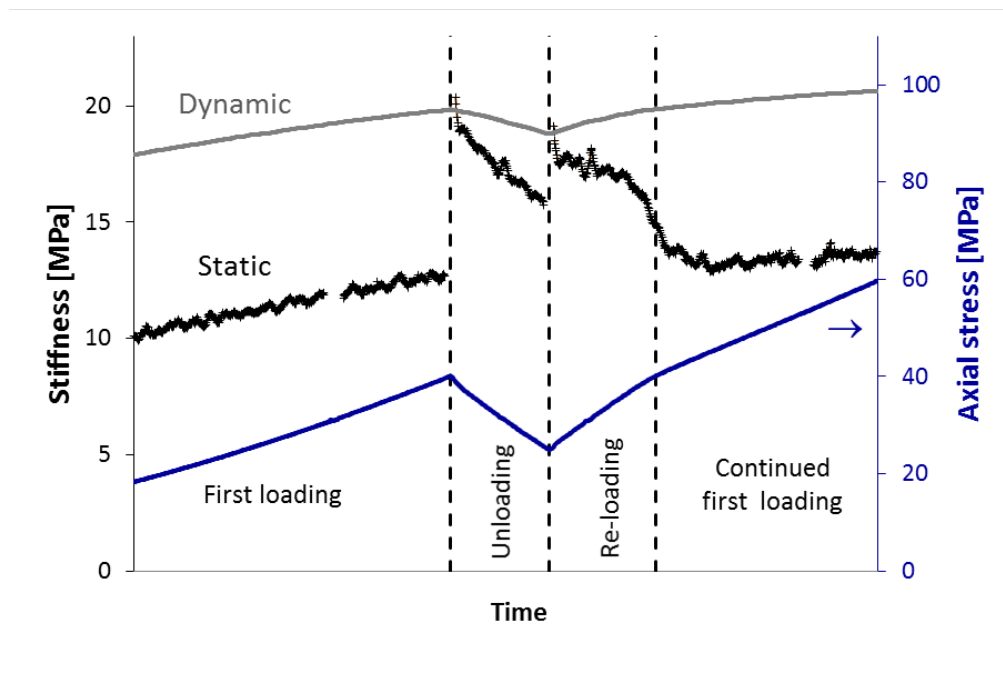


Figure 4

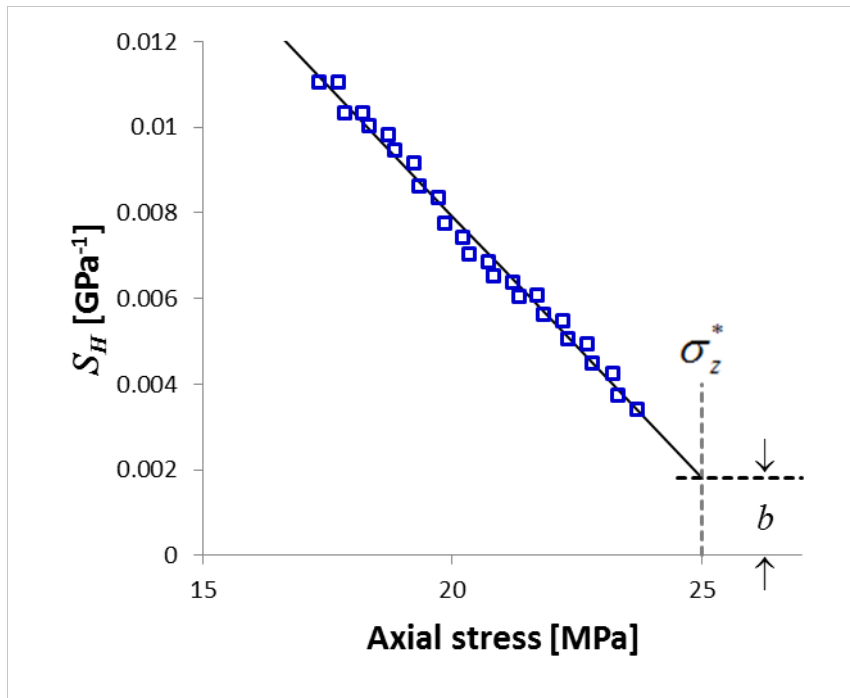


Figure 5